Faraday Discuss. Chem. Soc., 1983, **75**, 301–313

Unimolecular Decomposition of t-Butylhydroperoxide by Direct Excitation of the 6–0 O—H Stretching Overtone

By Mei-Chen Chuang, James E. Baggott,* David W. Chandler,†
William E. Farneth ‡ and Richard N. Zare §

Department of Chemistry, Stanford University, Stanford,
California 94305, U.S.A.

Received 16*th December*, 1982

The kinetics of the unimolecular decomposition of t-butylhydroperoxide [$(CH_3)_3COOH$] have been investigated when energy is deposited into 6 quanta of the O—H stretch, causing fission of the O—O bond. The 6–0 O—H overtone is pumped at 532 nm and the appearance of one of the ultimate products, t-butyl alcohol, is detected using optoacoustic spectroscopy to follow the reaction in situ. The results of the present work are compared with previous dissociation studies using direct overtone pumping at both 532 and 619 nm. The appearance rate of t-butyl alcohol as a function of pressure is not consistent with an R.R.K.M. treatment based on simple Stern–Volmer kinetics, but can be adequately fit by invoking collisional transfer to an electronic state, which decomposes more rapidly than the ground state, and/or invoking non-statistical behaviour.

One of the principal assumptions of statistical theories of unimolecular reactions, such as R.R.K.M. theory, is that intramolecular energy transfer occurs at a rate much faster than the chemical process involved (isomerisation, bond fission, etc.), such that the overall reaction rate is not governed by the *site* of energy deposition. Calculations are therefore performed without regard for site- or mode-selective behaviour.

The search for non-statistical or non-random effects in unimolecular processes has recently been stimulated by the technique of direct overtone excitation, introduced by Reddy and Berry.[1–4] They studied the dependence of the rate of isomerisation of methyl isocyanide [1–3] and allyl isocyanide [4] as a function of pressure, excitation energy and, for the latter molecule, the site of excitation. They reported that the rate of isomerisation of vibrationally excited allyl isocyanide did not conform to an R.R.K.M. analysis, but deviations from statistical behaviour were small.

In an attempt to provide less ambiguous evidence for non-statistical behaviour, this laboratory [5] studied the dissociation of t-butylhydroperoxide (t-BuOOH) induced by excitation of the 5–0 overtone of the O—H stretch at 619 nm, monitoring the rate of formation of one of the major stable products, t-butyl alcohol (t-BuOH), as a function of total pressure. Chandler et al.[5] obtained kinetic data which were found to be consistent with the reaction of a fraction (ca. 1%) of excited t-BuOOH molecules in which the excitation energy is non-randomly distributed. The data were fitted to a

* S.E.R.C. Postdoctoral Research Fellow.
† Present address: Combustion Research Facility, Sandia National Laboratory, Livermore, California 94550, U.S.A.
‡ Present address: Department of Chemistry, University of Minnesota, Minneapolis, Minnesota 55455, U.S.A.
§ Holder of a Shell Distinguished Chair, funded by the Shell Companies Foundation, Inc.

simple kinetic scheme suggesting rate constants of 10^9–10^{11} s^{-1} for dissociation from a non-statistical state distribution if the rate constant for energy randomisation within the molecule was taken to be in the range 10^{11}–10^{13} s^{-1}. The present work extends this original study to include excitation at 532 nm, corresponding to the 6–0 overtone of O—H stretch in t-BuOOH. The data from both studies are compared and discussed in terms of several kinetic schemes.

EXPERIMENTAL

The optoacoustic method provides quantitative in situ detection of t-BuOOH and its photolysis product t-BuOH.[5] Fig. 1 is a schematic diagram of the apparatus. A krypton

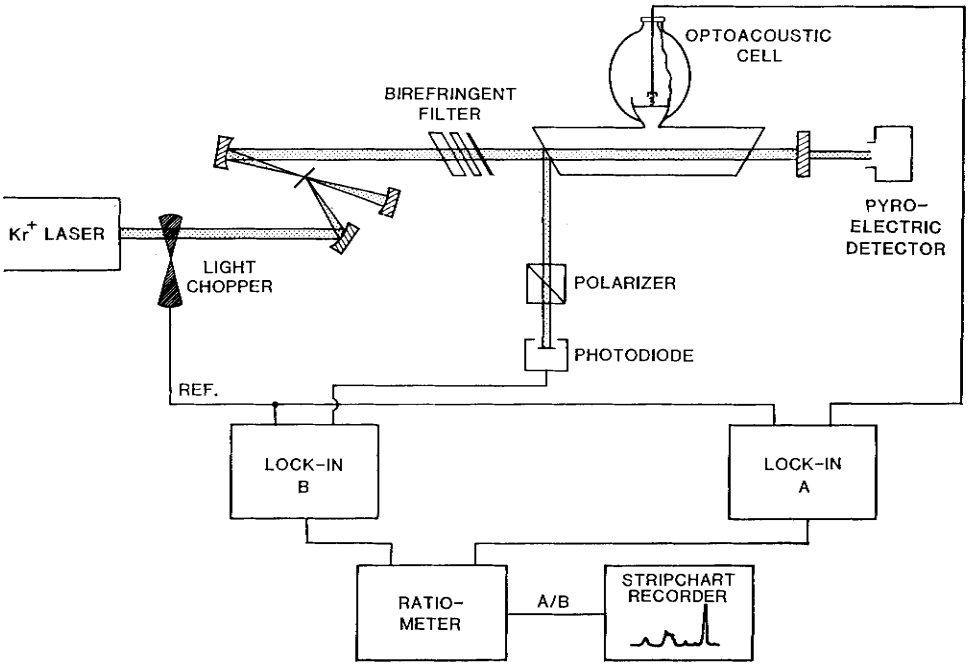

Fig. 1. Experimental arrangement. See text for details.

ion laser (Spectra Physics model 171–01), modulated at frequencies in the range 400–950 Hz, was used to pump a home-built linear dye laser [6] operating with Coumarin 515 in ethylene glycol. Small quantities of cyclooctatetraene were added to increase the dye laser power. The wavelength of the dye laser was tuned over the region 510–540 nm using a motor-driven three-plate birefrigent filter (Coherent Radiation) with a resolution of *ca.* 2 cm^{-1}. The intracavity dye laser power was monitored by reflection of light from one of the Brewster-angle windows of the reaction cell into a photodiode. During the photolysis, the laser power output through the end mirror was recorded using a pyroelectric detector. The response of this detector was calibrated to give the intracavity laser power using the known transmittance of the end mirror. Powers of typically 14–30 W were obtained.

The reaction cell, equipped with a one-inch condenser-type microphone (Brüel and Kjaer model 4144), was placed inside the dye-laser cavity. The optoacoustic and photodiode signals were processed by lock-in amplifiers (PAR model 163). The outputs from the amplifiers were ratioed (PAR model 193 ratiometer) and the resulting optoacoustic spectrum was displayed on a stripchart recorder. The reaction cell was passivated to reduce surface decomposition of t-BuOOH, as described previously.[5]

70% pure t-BuOOH was obtained from Aldrich and the water content reduced using anhydrous $MgSO_4$. Air was removed by exhaustive freeze–pump–thaw degassing. Fourier-transform infrared (f.t.i.r.) measurements on the resulting t-BuOOH samples revealed the presence of minor amounts of water and negligible amounts of acetone and t-BuOH.

RESULTS

OVERTONE SPECTRA

Fig. 2 shows the optoacoustic spectra of t-BuOOH and t-BuOH recorded in the 510–540 nm region. The assignments of the features were made previously [5] except for the peak at 536 nm which can be identified as the combination band of the 7–0 C—H stretch and the CC_3 deformation mode.

The v–0 transition energies of the O—H stretch and C—H stretch follow the relation [7]

$$E_{v-0} = v(A + vB) \tag{1}$$

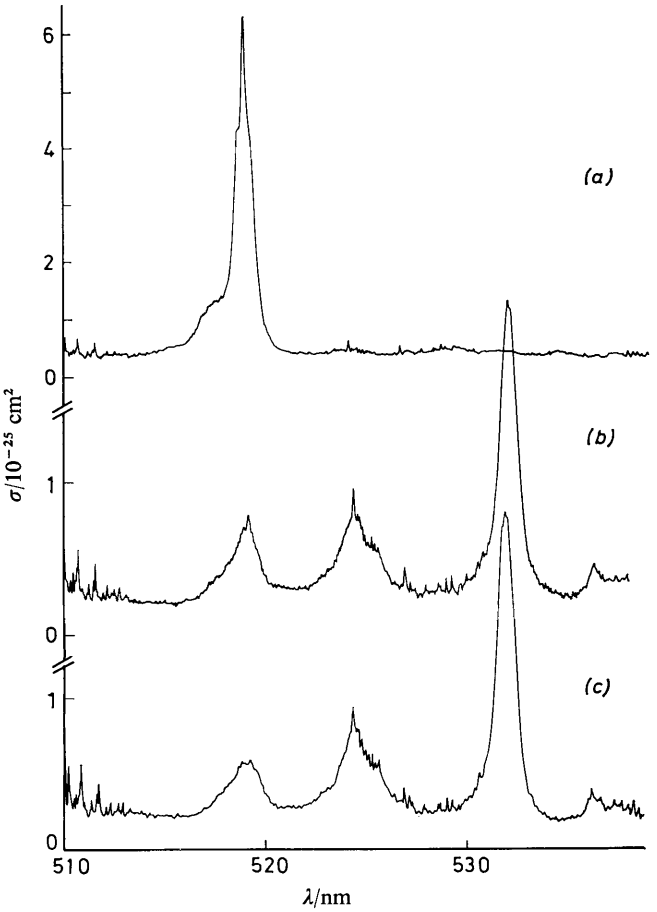

Fig. 2. Overtone spectra in the 510–540 nm region. (*a*), t-BuOH, showing the 6–0 O—H stretch absorption at 519 nm. (*b*), t-BuOOH after photolysis at 532 nm (ca. 1 h). The 6–0 O—H stretch absorption of the t-BuOH product is seen to grow in, superimposed upon the t-BuOOH combination band at 519 nm, when compared with (*c*), the overtone spectrum of t-BuOOH before photolysis. See ref. (5) for details of the assignment of the features.

where the constants A and B for the O—H stretch are 3692 cm^{-1} and -92.2 cm^{-1}, respectively; for the C—H stretch $A = 2985$ cm^{-1} and $B = -53.1$ cm^{-1}. Sharp lines in the spectra are recognised as water-vapour transitions.

Absolute absorption cross-sections for t-BuOOH and t-BuOH were calibrated against the known absolute absorption cross-section of the $6\nu_1 + \nu_3$ band of CH_4 at 543 nm.[8] In the earlier study of Chandler et al.[5] benzene vapour was used to calibrate the absorption cross-section of the 5–0 O—H stretch overtone in t-BuOOH at 619 nm. Unfortunately, benzene vapour could not be used as a reference standard in the present work owing to the overlap of the 7–0 C—H stretch absorption in C_6H_6 at 529 nm[9] with the 6–0 O—H stretch absorption in t-BuOOH at 532 nm. For similar reasons, CH_4 could not be used to calibrate the 5–0 O—H stretch absorption in t-BuOOH as the $5\nu_1 + \nu_3$ band of CH_4 is *centred* at 619 nm.[8] Comparison of the absorption strengths of C_6H_6 and CH_4 using the present arrangement indicates that the cross-sections for absorption into the 5–0 O—H and 6–0 O—H overtones in t-BuOOH may differ by approximately a factor of 5. However, the *absolute* values of the cross-sections are unlikely to be accurate to better than 50%. The fact that t-BuOOH may be adsorbed on the walls of the optoacoustic cell suggests that the cross-section reported in this work should be regarded as a lower limit.

TREATMENT OF KINETIC DATA

The method of data analysis used in the present work is similar to that described previously.[5] Fig. 2 shows that prolonged photolysis of t-BuOOH at 532 nm produces t-BuOH which can be observed by the growth of the t-BuOH 6–0 O—H stretch absorption, which is superimposed upon a combination band of t-BuOOH at 519 nm. Increases in the area of this band are therefore directly related to increases in the concentration of t-BuOOH formed in the reaction cell. In order to normalise the area with respect to variations in instrument response, measurements were made of the ratio, r, of the area of the superimposed t-BuOH 6–0 O—H stretch and t-BuOOH combination band at 519 nm relative to that of the 6–0 O—H stretch absorption in t-BuOOH at 532 nm. This ratio is given by

$$r = \frac{\alpha[\text{t-BuOH}]}{[\text{t-BuOOH}]} + \beta \qquad (2)$$

where α is a factor accounting for the different absorption cross-sections of t-BuOH and t-BuOOH in the wavelength regions of interest and β is the ratio of the integrated absorption cross-sections of the combination band and 6–0 O—H stretch in t-BuOOH.

In the analyses of the spectra, baselines were drawn by hand and peak areas were determined using a planimeter. The reproducibility of the measured peak ratios was assessed from analyses of several spectra taken consecutively. Some attempt was made to account for random error introduced by use of the planimeter by redetermining peak areas several times.

Despite efforts to passivate the walls of the reaction cell, surface decomposition of t-BuOOH still proceeded at a rate too fast to be neglected. The rate of production of t-BuOH due to this background reaction was therefore determined both before and after photolysis. Fig. 3 shows the results of a typical experiment. The actual rate of production of t-BuOH due to laser-induced decomposition of t-BuOOH was determined from

$$\frac{dr}{dt}(\text{laser-induced}) = \frac{dr}{dt}(\text{total}) - \frac{dr}{dt}(\text{background}). \qquad (3)$$

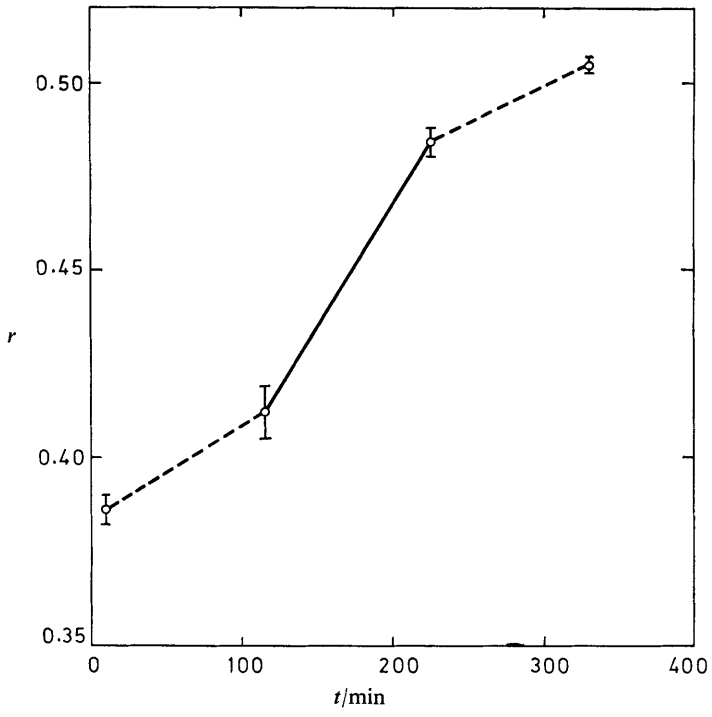

Fig. 3. Variation of the ratio of the area of the absorption band at 519 nm to that of the 6–0 O—H stretch absorption at 532 nm as a function of time. The solid line shows the increase in the ratio as a result of photolysis and the broken lines show the relative magnitude of the background dissociation of t-BuOOH. Experimental details: 7 Torr t-BuOOH at a total pressure of 150 torr (SF_6). Average intracavity laser power during photolysis was 21 W.

In the limit of very low conversion of t-BuOOH (conversions were typically $<5\%$):

$$\frac{dr}{dt} = \frac{\alpha \frac{d}{dt}[\text{t-BuOH}]}{[\text{t-BuOOH}]}. \tag{4}$$

As before,[5] the normalised rate constant for appearance of t-BuOH, k_{app}, was calculated from

$$k_{app} = \frac{\frac{d}{dt} r}{\alpha[h\nu]} \tag{5}$$

where $[h\nu]$ is the photon density in the reaction cell and is related to the magnitude of the pyroelectric detector signal. Thus,

$$k_{app} = \frac{\frac{d}{dt}[\text{t-BuOH}]}{[h\nu][\text{t-BuOOH}]}. \tag{6}$$

In fig. 4 the data obtained in the present work are presented together with data from the previous study in the form of plots of k_{app}^{-1} against pressure. In this study poor signal-to-noise ratios prevented the determination of k_{app} at pressures below 6

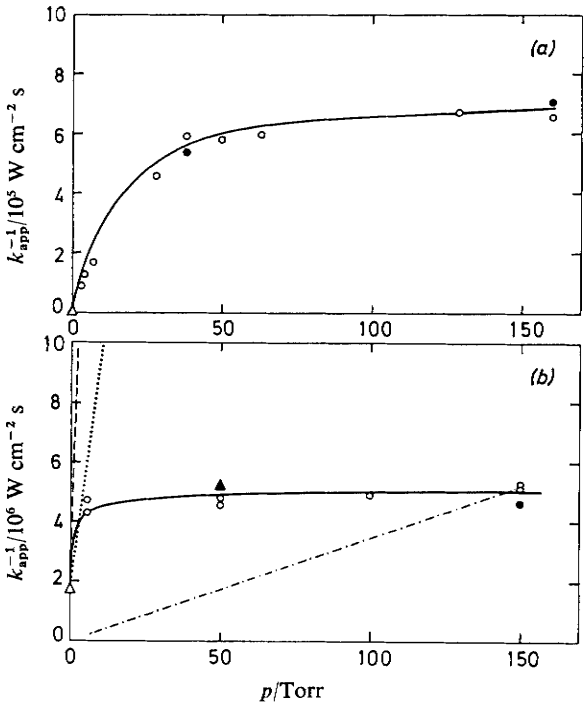

Fig. 4. (*a*) Variation of k_{app}^{-1} with total pressure for excitation at 619 nm, data taken from ref. (5). For pressures below 7 Torr pure t-BuOOH was used; ○, 7 Torr t-BuOOH + SF_6; ●, 1 Torr t-BuOOH + SF_6; △, calculated zero pressure intercept. The solid line shows the fit to the data provided by a kinetic scheme based on statistical and non-statistical energy distributions within reacting t-BuOOH† molecules, see ref. (5) for details. (*b*) Variation of k_{app}^{-1} with total pressure for excitation at 532 nm, obtained in the present study. Pure t-BuOOH was used for experiments at total pressures of 7 Torr. ○, 7 Torr t-BuOOH + SF_6; ●, 7 Torr t-BuOOH + Ar; ▲, data obtained in the presence of 15 Torr of 1,4-cyclohexadiene; △, calculated zero pressure intercept. Average error in the experimental data is estimated to be ±15%. (– – – –) Variation predicted on the basis of a simple single-collision Stern–Volmer analysis, scheme I. (· · · ·) Analysis using a mechanism which allows for the effects of weak collisions, see text. (– · – ·) Analysis using scheme II, allowing for complications arising from secondary free radical chemistry. (——) Predicted variation based on either scheme III, invoking reaction from t-BuOOH† molecules with statistical and non-statistical energy distributions, or scheme IV, collision-induced formation of a dissociative electronic state of t-BuOOH.

Torr.* Checks were made to ensure that the values of k_{app} obtained were independent of the intracavity laser power. Photolysis at wavelengths not corresponding to absorption by t-BuOOH produced no reaction above that attributable to surface decomposition, as indicated by analyses of the overtone spectra and by f.t.i.r. spectroscopy.

Other possible experimental artifacts such as laser-induced heating of the sample, reaction at the windows of the cell and two-photon absorption have been considered in connection with an earlier investigation,[5] and reference is made here to the arguments presented in that work.

* 1 Torr ≡ 101 325/760 Pa.

DISCUSSION

STERN–VOLMER MECHANISM

The simplest kinetic scheme that can be constructed for the dissociation of t-BuOOH following overtone excitation is a Stern–Volmer mechanism (scheme I):

$$h\nu + \text{t-BuOOH} \xrightarrow{k_1} \text{t-BuOOH}\,\dagger \qquad \text{(R1)}$$

$$\text{t-BuOOH}\,\dagger \xrightarrow{k_2} \text{t-BuO} + \text{OH} \qquad \text{(R2)}$$

$$\text{t-BuOOH}\,\dagger + \text{M} \xrightarrow{k_3} \text{t-BuOOH} + \text{M} \qquad \text{(R3)}$$

$$\text{t-BuO} + \text{t-BuOOH} \xrightarrow{k_4} \text{t-BuOH} + \text{t-BuOO} \qquad \text{(R4)}$$

$$\text{OH} + \text{t-BuOOH} \xrightarrow{k_5} \text{H}_2\text{O} + \text{t-BuOO} \qquad \text{(R5)}$$

$$\text{t-BuOO} \xrightarrow{k_6} \text{termination} \qquad \text{(R6)}$$

where t-BuOOH † represents a vibrationally excited molecule and M a bath gas molecule. Steady-state analysis of scheme I predicts

$$\frac{\mathrm{d}}{\mathrm{d}t}[\text{t-BuOH}] = \frac{k_1 k_2 [h\nu][\text{t-BuOOH}]}{k_2 + k_3[\text{M}]}. \qquad (7)$$

Comparison with eqn (6) shows that

$$k_{\text{app}} = \frac{k_1 k_2}{k_2 + k_3[\text{M}]}. \qquad (8)$$

This simple scheme therefore predicts that k_{app}^{-1} should depend linearly upon the total pressure, [M], with an intercept of $1/k_1$ and a slope of k_3/k_1k_2. The rate constant k_1 was calculated by assuming $k_1 = \sigma c$, where σ is the absorption cross-section of t-BuOOH at 532 nm and c is the speed of light. For comparison with the experimental data, which were determined in units of $\text{cm}^2\ \text{W}^{-1}\ \text{s}^{-1}$ the relation $k_1 = \sigma/h\nu$ is appropriate, and yields a value of $6.0 \times 10^{-7}\ \text{cm}^2\ \text{W}^{-1}\ \text{s}^{-1}$. It should be recalled, however, that σ is unlikely to be known accurately to better than 50%, placing a correspondingly large uncertainty on the calculated value of k_1.

Evaluation of eqn (8) requires values for k_2 and k_3. Experimental values for these rate constants have been provided by the study of the unimolecular dissociation of t-BuOOH excited at 532 nm conducted by Rizzo and Crim.[10] They derived $k_2 = 4 \times 10^6\ \text{s}^{-1}$ and $k_3 = 2.5 \times 10^{-10}\ \text{cm}^3\ \text{molecule}^{-1}\ \text{s}^{-1}$ from the exponential rise of OH laser-induced fluorescence following dissociation, in agreement with previous calculations.[5] Use of these values for k_1, k_2 and k_3 in eqn (8) leads to the prediction of a strong dependence of k_{app}^{-1} on pressure, as indicated by the dashed line of fig. 4(*b*). The data clearly do not conform to the dependence predicted by this simple analysis.

In the following, several mechanistic schemes are considered which might cause deviations from the behaviour discussed above. These are concerned with the many assumptions that have been made in writing scheme I.

THERMAL DISTRIBUTION OF ACTIVATED MOLECULES

Earlier work [5] showed that the *distribution* of internal energies of the activated molecules can make a significant difference to the expected slope (and curvature) of

the Stern–Volmer plot. In these considerations k_2 is identified not as $k_2(\bar{E})$, where $\bar{E}$ is the mean of the energy distribution, but as a function of E. Then k_{app} is given by

$$k_{app} = k_1 \int_{E=h\nu}^{\infty} \frac{k_2(E)}{k_2(E) + k_3[M]} f(E)dE \qquad (9)$$

where $f(E)$ is the energy distribution obtained as a result of excitation. However, in the present study, excitation at 532 nm generates a distribution of activated molecules within an energy range in which $k_2(E)$ varies more slowly with E than is the case for 619 nm excitation [cf. fig. 8 of ref. (5)]. The effects of reaction of a distribution of energised molecules will thus be smaller for the higher energy excitation, and the variation of k_{app}^{-1} with pressure predicted by eqn (9) is not expected to be significantly different from the dependence given by the dashed line in fig. 4(*b*).

EFFECTS OF WEAK COLLISIONS

In scheme I it has been assumed that in every collision between t-BuOOH † and a bath gas molecule sufficient energy is transferred from the activated species to make it effectively unreactive. For example, if the energy transferred per collision is of the order of 2000 cm^{-1}, the calculated R.R.K.M. rate constant falls by more than an order of magnitude.[5] Recent studies, both theoretical [11] and experimental [12–15] have indicated that in the limit of " weak " collisions, the average energy transferred per collision is likely to be much less than 2000 cm^{-1}. Thus, given the high excitation energy of the present work the possibility that *several* collisions may be required to deactivate completely the initially prepared t-BuOOH † species should be considered. It has been recognised [16] that neglect of weak collisional effects can lead to the overestimation of unimolecular reaction rate constants obtained from analyses based on single-collision Stern–Volmer mechanisms.

In the limit that $k_3[M]/\{k_2(\bar{E}) + k_3[M]\}$ approaches unity, it can be shown that

$$k_{app} = \frac{k_1}{k_2(\bar{E}_1) + k_3[M]} \{k_2(\bar{E}_1) + k_2(\bar{E}_2) + k_2(\bar{E}_3) \ldots + k_2(\bar{E}_n)\} \qquad (10)$$

where $\bar{E}_1$, $\bar{E}_2$, $\bar{E}_3 \ldots \bar{E}_n$ represents the average energy content of t-BuOOH † following successive collisions. In obtaining eqn (10) it has been assumed that the collision rate constant, k_3, is unaffected by the energy content of the molecule. Calculations based on eqn (10) were performed using a value for the average energy transferred per collision of 100 cm^{-1}. This corresponds to a weak collision limit with ca. $n = 50$ collisions required to deactivate completely the t-BuOOH † molecules. Values for $k_2(\bar{E})$ based on R.R.K.M. calculations [5] were assumed. The results are shown in fig. 4(*b*) as the dotted line.

Such a calculation assumes many simplifications with regard to the changes in the form of the energy distribution, $f(E)$, following successive collisions, and should be regarded as a crude picture based on assumed properties of the *average* photoactivated molecule. Nevertheless, the results should be qualitatively correct. A reduction in the magnitude of the slope of the Stern–Volmer plot is indicated but it is very difficult to see how weak collision effects can lead to a pressure-independent k_{app}^{-1}. Furthermore, such an explanation suggests that k_{app}^{-1} should depend sensitively on the nature of the bath gas molecules, whereas the data in fig. 4(*b*) reveal that k_{app}^{-1} is independent of the collision partners t-BuOOH, SF_6 and Ar. It is concluded, therefore, that inefficient collisional energy transfer cannot explain the experimentally observed pressure dependence of k_{app}^{-1}.

SECONDARY RADICAL REACTIONS

The t-BuO radical formed as a result of dissociation of t-BuOOH may react in a manner other than indicated by reaction (R4). In particular, small quantities of acetone were observed using f.t.i.r. spectroscopy following the decomposition of t-BuOOH at 7 Torr total pressure. No acetone could be observed at high pressures (600 Torr), suggesting that formation of this product is pressure-dependent. Acetone is a decomposition product of the t-BuO radical:

$$\text{t-BuO} \rightarrow (\text{CH}_3)_2\text{CO} + \text{CH}_3. \qquad \text{(R7)}$$

In addition, reaction (R6) has assumed that the only fate of the t-BuOO radicals produced via reactions (R4) and (R5) is termination (presumably) on the walls of the reaction cell.[5] In the absence of such terminating reactions, the likely fate of t-BuOO radicals is recombination:

$$2\text{t-BuOO} \rightarrow 2\text{t-BuO} + \text{O}_2. \qquad \text{(R8)}$$

Note, however, that not all recombination is thought to lead to chain propagation in this way; Kirsch and Parkes [17] have presented evidence to suggest that some di-t-butyl peroxide is formed in a homogeneous termination process. For the purposes of the present discussion it will be assumed that *all* t-BuOO recombination leads to propagation. Scheme II, which includes these other chemical processes, can thus be written:

$$h\nu + \text{t-BuOOH} \xrightarrow{k_1} \text{t-BuOOH}\,\dagger \qquad \text{(R1)}$$

$$\text{t-BuOOH}\,\dagger \xrightarrow{k_2} \text{t-BuO} + \text{OH} \qquad \text{(R2)}$$

$$\text{t-BuOOH}\,\dagger + \text{M} \xrightarrow{k_3} \text{t-BuOOH} + \text{M} \qquad \text{(R3)}$$

$$\text{t-BuO} + \text{t-BuOOH} \xrightarrow{k_4} \text{t-BuOH} + \text{t-BuOO} \qquad \text{(R4)}$$

$$\text{OH} + \text{t-BuOOH} \xrightarrow{k_5} \text{H}_2\text{O} + \text{t-BuOO} \qquad \text{(R5)}$$

$$\text{t-BuO} \xrightarrow{k_7} (\text{CH}_3)_2\text{CO} + \text{CH}_3 \qquad \text{(R7)}$$

$$2\text{t-BuOO} \xrightarrow{k_8} 2\text{t-BuO} + \text{O}_2. \qquad \text{(R8)}$$

Scheme II features these secondary reactions in such a way that they should exert their greatest possible influence upon the rate of production of t-BuOH, consistent with deviations from the simple Stern–Volmer behaviour of scheme I. A steady-state analysis of this scheme gives

$$k_{\text{app}}^{-1} = \frac{k_7(k_2 + k_3[\text{M}])}{2k_1k_2k_4[\text{t-BuOOH}]}. \qquad (11)$$

This expression can be fitted to the data obtained at 150 Torr using $k_1 = 6.0 \times 10^{-7}$ cm^2 W^{-1} s^{-1}, $k_2 = 4 \times 10^6$ s^{-1} and $k_3 = 2.5 \times 10^{-10}$ cm^3 molecule^{-1} s^{-1}, if the ratio $(k_7/k_4[\text{t-BuOOH}])$ is assumed to be 4.2×10^{-3}, i.e. if k_7/k_4 is assumed to be 9.5×10^{14} molecule cm^{-3} for t-BuOOH pressures of 7 Torr. This last figure should be compared with the value of 5×10^{14} molecule cm^{-3} reported for k_7/k_4 by Kirsch and Parkes.[17] Use of the value of k_7/k_4 derived by fitting eqn (11) to the data at 150 Torr gives the predicted pressure dependence of k_{app}^{-1} as shown by the dot-dashed curve in fig. 4(*b*), i.e. a significant pressure dependence is obtained. Note, however, that scheme II does not predict a variation with pressure for the rate of production of

acetone *relative* to that of t-BuOH, as observed experimentally. It is possible that acetone formation is governed by decomposition of t-BuO radicals which possess some internal excitation following O—O bond cleavage in t-BuOOH†. Such excited t-BuO radicals will be quenched by collisions with bath-gas molecules at rates similar in magnitude to the quenching of t-BuOOH † itself, resulting in slower acetone formation rates at higher pressures. However, at the lowest pressures studied, acetone accounted for no more than ca. 15% of the total carbon-containing product yield, t-BuOH being the major product of this type.

These considerations suggest that complications arising from post-dissociation free-radical chemistry are unlikely to affect significantly the *form* of the dependence of k_{app}^{-1} on pressure, at least, not to the extent that k_{app}^{-1} would be predicted to become pressure-independent. As discussed previously,[5] such expectations are consistent with a simple consideration of the relative magnitudes of the reaction rate constants involved; in the presence of significant quantities of t-BuOOH the abstraction reactions (R4) and (R5) are anticipated to dominate any other reactive channel involving t-BuO and OH radicals.[17,18]

The absence of interfering effects arising from t-BuOO recombination was demonstrated experimentally by the addition of an excess of the H-atom donor 1,4-cyclohexadiene. The reaction

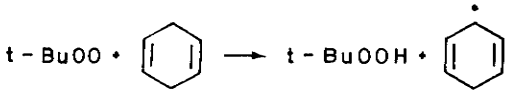

(R9)

is more exothermic than t-BuOO recombination by ca. 51 kJ mol^{-1} [ref. (5)], and at the concentration levels of 1,4-cyclohexadiene used reaction (R9) should be the principal pathway for the removal of t-BuOO. Thus, if reaction (R8) were an important contributor to the overall production of t-BuOH, the removal of t-BuOO via reaction (R9) would be expected to be reflected in the measured value of k_{app}^{-1}. At 50 Torr total pressure, no variation in k_{app}^{-1} was obtained on addition of 15 Torr of 1,4-cyclohexadiene [see fig. 4(*b*)].

We conclude that secondary radical reactions are not responsible for the form of the dependence of k_{app}^{-1} upon pressure obtained experimentally, although some complications arising from the decomposition of activated t-BuO radicals may affect the data at low pressures.

NON-STATISTICAL BEHAVIOUR

The pressure dependence of k_{app}^{-1} for excitation of t-BuOOH at 619 nm was suggested by Chandler et al.[5] to be consistent with a mechanistic scheme involving decomposition from excited t-BuOOH molecules in which the energy is distributed non-randomly, violating one of the principal assumptions of R.R.K.M. theory. This type of scheme, which has been used principally by Rabinovitch and co-workers [19,20] to rationalise chemical activation data, can be written as scheme III:

$$h\nu + \text{t-BuOOH} \xrightarrow{k_{10}} \text{t-BuOOH}\,\dagger\dagger \qquad \text{(R10)}$$

$$\text{t-BuOOH}\,\dagger\dagger \xrightarrow{k_{11}} \text{t-BuO} + \text{OH} \qquad \text{(R11)}$$

$$\text{t-BuOOH}\,\dagger\dagger \xrightarrow{k_{12}} \text{t-BuOOH}\,\dagger \qquad \text{(R12)}$$

$$\text{t-BuOOH}\,\dagger \xrightarrow{k_2} \text{t-BuO} + \text{OH} \qquad \text{(R2)}$$

$$\text{t-BuOOH}\,\dagger + \text{M} \xrightarrow{k_3} \text{t-BuOOH} + \text{M} \qquad \text{(R3)}$$

$$\text{t-BuO} + \text{t-BuOOH} \xrightarrow{k_4} \text{t-BuOH} + \text{t-BuOO} \qquad \text{(R4)}$$

in which t-BuOOH †† represents an activated t-BuOOH molecule in which the excitation energy is not totally randomised. Analysis of this scheme gives

$$k_{\text{app}} = k_{10}\left(\frac{k_2}{(k_2 + k_3[\text{M}])}\,\frac{k_{12}}{k_{11} + k_{12}} + \frac{k_{11}}{k_{11} + k_{12}}\right). \qquad (12)$$

In the limit $k_3[\text{M}] \gg k_2$, corresponding to relatively high pressures, k_{app}^{-1} tends to the value

$$k_{\text{app}}^{-1} = \frac{k_{11} + k_{12}}{k_{10}k_{11}} \qquad (13)$$

assuming that k_{11} and k_{12} are of similar orders of magnitude. Eqn (13) shows that k_{app}^{-1} becomes independent of pressure at a value determined by the fraction $k_{11}/(k_{11} + k_{12})$.

The data obtained for excitation of t-BuOOH at 619 nm, shown in fig. 4(*a*), were found [5] to be consistent with scheme III assuming a value of ca. 0.01 for $k_{11}/(k_{11} + k_{12})$. Rate constants for energy randomisation [reaction (R12)] of the order of 10^{11}–10^{13} s^{-1} have been indicated by the results of chemical activation experiments.[20] Combination of this range of values for k_{12} with the value given above for $k_{11}/(k_{11} + k_{12})$ suggests values for k_{11} in the range 10^9–10^{11} s^{-1}. It was shown [5] that dissociation rate constants in this range could be reproduced by calculations based on R.R.K.M. theory in which the excitation energy was assumed to be localised within a reasonable " part-molecule ". For example, calculations utilising an activated molecule which does not include oscillators and rotors involving CH and which ignores C—C stretches (leaving 12 internal degrees of freedom) predict a value for k_{11} of 3×10^9 s^{-1}, which we denote by $k_{11}(\text{P}_1)$. The assumption that the energy is localised only in oscillators within the C—O—O—H group leads to a value for $k_{11}(\text{P}_2)$ of ca. 1×10^{11} s^{-1}.

The data of fig. 4(*b*) suggest that for 532 nm excitation the fraction $k_{11}/(k_{11} + k_{12})$ becomes ca. 0.34 [solid line in fig. 4(*b*)]. Note, however, that this fraction is fixed by the calculated value of k_{10} (taken to be equal to k_1) and is subject to considerable uncertainty. Combination of this value for $k_{11}/(k_{11} + k_{12})$ with values for k_{12} in the range 10^{11}–10^{13} s^{-1} suggests values for k_{11} in the range (5×10^{10})–(5×10^{12}) s^{-1}. Similar part-molecule calculations were performed for 532 nm excitation and were found to yield values for $k_{11}(\text{P}_1)$ of 4×10^{10} s^{-1} and $k_{11}(\text{P}_2)$ of 3×10^{12} s^{-1}.

These arguments demonstrate that within the framework of scheme III, the data sets of fig. 4(*a*) and (*b*) are compatible. Unfortunately, owing to the uncertainty of the calculated value of k_1, the amount of non-statistical chemistry that must be invoked to explain the data of fig. 4(*b*) cannot be determined accurately at the present time.

The only other experimental information available comes from the time-resolved studies of Rizzo and Crim.[10] They observed the growth and decay of OH laser-induced fluorescence (l.i.f.) intensity resulting from the photodissociation of t-BuOOH at 532 nm. It would seem from fig. 1(*a*) of ref. (10) that a significant amount of l.i.f. intensity (ca. 20% of the total) is seen at the very shortest delay times, suggesting that some dissociation might be occurring on a collision-free timescale. More recent experiments indicate that this fraction may be 10% or smaller.[21]

DISSOCIATION FROM AN EXCITED ELECTRONIC STATE

The relatively high level of excitation used in the present work suggests that the proximity of possible low-lying excited electronic states within t-BuOOH should be

considered. In particular, the combination of t-BuO and OH radicals can take place on an associative singlet surface (leading to ground-state t-BuOOH) or a repulsive triplet surface. This latter surface will thus be associated with high energy levels of the reaction coordinate for t-BuOOH dissociation. Reaction from a dissociative state would be expected to proceed on a timescale much shorter than that for collisional quenching, and can explain the data if it is assumed that the state is formed via collisions (either up-pumping collisions or simply encounters which provide suitable perturbation of the initially prepared t-BuOOH †). This is represented by scheme IV:

$$h\nu + \text{t-BuOOH} \xrightarrow{k_1} \text{t-BuOOH}\,\dagger \qquad \text{(R1)}$$

$$\text{t-BuOOH}\,\dagger \xrightarrow{k_2} \text{t-BuO} + \text{OH} \qquad \text{(R2)}$$

$$\text{t-BuOOH}\,\dagger + \text{M} \xrightarrow{k_3} \text{t-BuOOH} + \text{M} \qquad \text{(R3)}$$

$$\text{t-BuOOH}\,\dagger + \text{M} \xrightarrow{k_{13}} \text{t-BuOOH*} + \text{M} \qquad \text{(R13)}$$

$$\text{t-BuOOH*} \xrightarrow{k_{14}} \text{t-BuO} + \text{OH} \qquad \text{(R14)}$$

$$\text{t-BuO} + \text{BuOOH} \xrightarrow{k_4} \text{t-BuOH} + \text{t-BuOO} \qquad \text{(R4)}$$

where t-BuOOH* represents an electronically excited molecule. Analysis of scheme IV gives

$$k_{\text{app}}^{-1} = \frac{k_2 + (k_3 + k_{13})[\text{M}]}{k_1(k_2 + k_{13}[\text{M}])} \qquad (14)$$

and predicts that at high pressures k_{app}^{-1} should tend to a limiting value given by

$$k_{\text{app}}^{-1} = \frac{k_3 + k_{13}}{k_1 k_{13}} \qquad (15)$$

assuming $k_{13}[\text{M}] \gg k_2$. This limiting high-pressure value predicted for k_{app}^{-1} is independent of pressure, its absolute value being determined by the relative magnitudes of k_3 and k_{13}. The solid line drawn through the data of fig. 4(*b*) can be reproduced by assuming the usual values for k_1 and k_2 and a branching ratio of 34% for collisional formation of the state t-BuOOH*, which represents an upper limit.

Thus analysis in terms of scheme IV predicts a strong dependence upon pressure for k_{app}^{-1} at total pressures below ca. 6 Torr. Above this pressure the collisional route to t-BuOOH† dissociation dominates the direct dissociation step. Only one experimental observation can be used in argument against such a mechanism: k_{app}^{-1} was found to be independent of the identity of the bath-gas molecule, t-BuOOH, SF_6 or Ar. The limiting high pressure expression for k_{app}^{-1} contains the rate constants k_3 and k_{13}, both of which might be expected to be sensitive to the identity of the bath gas, particularly if reaction (R13) involves intersystem crossing. However, in the absence of further experimental information, collision-induced dissociation of t-BuOOH† via some intermediate electronic state remains a possibility which we cannot exclude.

CONCLUDING REMARKS

Dissociation of t-BuOOH via overtone excitation at 619 nm was shown [5] to exhibit behaviour which is consistent with a mechanism involving reaction of a fraction of excited molecules with non-random energy distributions. However, the effects were

small (ca. 1% of the total decomposition) and the possibility that such behaviour was explicable in terms of a minor, pressure-independent reaction channel could not be excluded.

In the present work, the kinetic data reveal major deviations between a simple Stern–Volmer analysis and the observed behaviour, indicating drastic differences in the mechanism of dissociation. The effects are much more pronounced and minor reaction pathways can no longer be responsible.

Whatever the origin of the observed unimolecular decomposition rates, the data cannot be reconciled with the previous wisdom of Stern–Volmer kinetics and statistical energy randomisation. This paradigm fails but we are uncertain as to what new paradigm will suffice. The possibility that the observed data can be explained in terms of decomposition of energised t-BuOOH †† in which energy randomisation is incomplete is attractive, but we cannot exclude other possibilities, such as collisional transfer to a state that rapidly dissociates.

We acknowledge the support of the National Science Foundation under grant NSF CHE 80–06524.

[1] K. V. Reddy and M. J. Berry, *Chem. Phys. Lett.*, 1977, **52**, 111.
[2] K. V. Reddy, R. G. Bray and M. J. Berry, in *Advances in Laser Chemistry*, ed. A. H. Zewail (Springer-Verlag, Berlin, 1978).
[3] K. V. Reddy and M. J. Berry, *Faraday Discuss. Chem. Soc.*, 1979, **67**, 188.
[4] K. V. Reddy and M. J. Berry, *Chem. Phys. Lett.*, 1979, **66**, 223.
[5] D. W. Chandler, W. E. Farneth and R. N. Zare, *J. Chem. Phys.*, 1982, **77**, 4447.
[6] L. Wöste, *Ph.D. Thesis* (University of Bern, Switzerland, 1978).
[7] R. L. Swofford, M. E. Long and A. C. Albrecht, *J. Chem. Phys.*, 1976, **62**, 179.
[8] L. P. Giver, *J. Quant. Spectrosc. Radiat. Transfer*, 1978, **19**, 311.
[9] K. V. Reddy, D. F. Heller and M. J. Berry, *J. Chem. Phys.*, 1982, **76**, 2814.
[10] T. R. Rizzo and F. F. Crim, *J. Chem. Phys.*, 1982, **76**, 2754.
[11] J. Troe, *J. Chem. Phys.*, 1982, **77**, 3485.
[12] D. L. Tardy and B. S. Rabinovitch, *Chem. Rev.*, 1977, **77**, 369.
[13] H. Hippler, J. Troe and H. J. Wendelken, presented at the *7th International Symposium on Gas Kinetics*, Göttingen, August 1982.
[14] M. J. Rossi and J. R. Barker, *Chem. Phys. Lett.*, 1982, **85**, 21.
[15] J. R. Barker, M. J. Rossi and J. R. Pladziewicz, presented at the *7th International Symposium on Gas Kinetics*, Göttingen, August 1982.
[16] G. H. Kohlmaier and B. S. Rabinovitch, *J. Chem. Phys.*, 1963, **38**, 1692; R. Walsh, *Faraday Discuss. Chem. Soc.*, 1979, **67**, 237.
[17] L. J. Kirsch and D. A. Parkes, *J. Chem. Soc., Faraday Trans. 1*, 1981, **77**, 293.
[18] C. Anastasi, I. W. M. Smith and D. A. Parkes, *J. Chem. Soc., Faraday Trans. 1*, 1978, **74**, 1693.
[19] A-N. Ko and B. S. Rabinovitch, *Chem. Phys.*, 1978, **30**, 361.
[20] I. Oref and B. S. Rabinovitch, *Acc. Chem. Res.*, 1979, **12**, 166.
[21] F. F. Crim, personal communication, 1982.